Microscale tracking of coral disease reveals timeline of infection and heterogeneity of polyp fate.

Assaf R. Gavish[1], Orr H. Shapiro[1,2,*], Esti Kramarsky-Winter[1] and Assaf Vardi[1]*

[1]Department of Plant and Environmental Sciences, Weizmann Institute of Science, Rehovot, Israel.

[2]Department of Food Quality and Safety, Agricultural Research Organization, Volcani Center, Rishon LeZion, Israel.

* –Corresponding authors: orr@agri.gov.il, assaf.vardi@weizmann.ac.il

Abstract

Coral disease is often studied at scales ranging from single colonies to the entire reef. This is particularly true for studies following disease progression through time. To gain a mechanistic understanding of key steps underlying infection dynamics, it is necessary to study disease progression, and host-pathogen interactions, at relevant microbial scales. Here we provide a dynamic view of the interaction between the model coral pathogen *Vibrio coralliilyticus* and its coral host *Pocillopora damicornis* at unprecedented spatial and temporal scales. This view is achieved using a novel microfluidics-based system specifically designed to allow microscopic study of coral infection *in-vivo* under controlled environmental conditions. Analysis of exudates continuously collected at the system's outflow, allows a detailed biochemical and microbial analyses coupled to the microscopic observations of the disease progression. The resulting multilayered dataset provides the most detailed description of a coral infection to-date, revealing distinct pathogenic processes as well as the defensive behavior of the coral host. We provide evidence that infection in this system occurs following ingestion of the pathogen, and may then progress through the gastrovascular system. We further show infection may spread when pathogens colonize lesions in the host tissue. Copious spewing of pathogen-laden mucus from the polyp mouths results in effective expulsion of the pathogen from the gastrovascular system, possibly serving as a first line of defense. A secondary defense mechanism entails the severing of calicoblastic connective tissues resulting in the controlled isolation of diseased polyps, or the survival of individual polyps within infected colonies. Further investigations of coral-pathogen interactions at these scales will help to elucidate the complex interactions underlying coral disease, as we as the versatile adaptive response of the coral ecosystems to fluctuating environments.

Introduction

Coral reefs are currently undergoing an unprecedented decline driven by local and global changes to their environment[1]. Reef building corals, commonly described as holobionts, form a complex relationship with photosynthesizing dinoflagellates (*Symbiodinium spp.*) and a consortium of microbial partners[2]. Shifts in environmental conditions may lead to the breakdown of these symbiotic relations, often with catastrophic consequences for the coral colony. Such processes, collectively termed coral disease[3, 4], may be manifested as a loss of the algal symbionts (coral bleaching)[5], or as damage to the coral colony due to various forms of necrotic loss of coral tissue[2]. On large scales, these processes may result in loss of coral cover, ultimately leading to the degradation of the reef structure and the loss of associated ecological and societal services[4, 6, 7].

Many coral diseases are linked to specific pathogens whose abundance and virulence increase in response to environmental changes. Such changes may include nutrient loading, pollution, and temperature shifts[8-11]. One of the best characterized coral diseases is the infection of the Indo-Pacific coral *Pocillopora damicornis* by the bacterial pathogen *Vibrio coralliilyticus*[9, 12, 13]. The virulence of *V. coralliilyticus* is known to be positively correlated with increased temperatures[9, 14-16]. Increased ambient temperatures are further linked to accelerated vibrio growth rates[9], enhanced chemotaxis and chemokinesis[17], and secretion of matrix metalloproteases (MMPs)[18]. Nevertheless, a mechanistic understanding linking these traits to coral infection and disease progress is still lacking.

Many coral disease studies focus on monitoring coral colonies for the appearance of macroscopic signs of disease. These may include various forms of tissue discoloration, loss of the algal symbionts, or loss of tissue integrity[19, 20]. This tendency for macroscale studies is derived to a large extent from the complexity of the coral holobiont[21, 22], and the difficulty in establishing a tractable model system facilitating more detailed observations[22, 23]. Currently, the main available tool enabling to link a potential pathogen to the site of tissue damage and to the host

response is histopathology[23]. However, as such disease manifestations only appear at advanced stages of the infection process, their use as disease indicators fails to capture the early stages of pathogen colonization and disease initiation[23]. We are thus lacking a mechanistic understanding of key steps in the infection process, including e.g. site of initial colonization, possible functions of specific disease markers such as MMP's, or where bacterial chemotaxis may come into play. Furthermore, there are still major knowledge gaps in our understanding of coral response at the onset of pathogenic infection.

Here we present a new microfluidic system, the Microfluidic Coral Infection (MCI) platform, developed specifically to tackle question related to the interaction between a bacterial pathogen and a coral colony at high spatio-temporal resolutions. This platform has several features distinguishing it from the previously published coral-on-a-chip (CoC) system[24]. The larger chamber volume and higher flow rates of the MCI, as compared to the CoC, facilitate the incubation of small coral fragments, preserving the colonial morphology of the coral colony. Moreover, the MCI design allows the continuous collection of exudates of the system for downstream analysis. The MCI further allows the incubation and tracking of up to 6 individual coral fragments in separate chambers, facilitating flexible experimental design. Using the MCI system we track the microscopic encounter between the bacterial pathogen *V. coralliilyticus* and its coral host *P. damicornis.* Coupling the resulting time-lapse microscopic imaging with biochemical and microbial analyses of the system's outflow we identify early stages of the infection process that were not previously described. These results bring us a step closer towards a mechanistic understanding of microbial disease processes in reef building corals.

Results

Live imaging of coral infection

The progression of bacterial infection of small coral fragments was enabled using the MCI platform (Figure 1; Supplementary figure 1). To demonstrate the

92 robustness of this system, healthy *P. damicornis* fragments were incubated under
93 controlled environmental conditions (temperature, light, flow, and water quality).
94 Tissue integrity was continuously monitored by microscopic imaging. Natural coral
95 Green Fluorescence Protein (GFP) served as a biomarker for coral health, while
96 chlorophyll autofluorescence served to track localization and wellbeing of its
97 zooxanthellae symbionts. No changes in coral morphology or behavior, and no
98 extensive loss of algal symbionts (bleaching) were observed following 48 h of
99 incubation under constant flow of filtered artificial seawater (FASW).

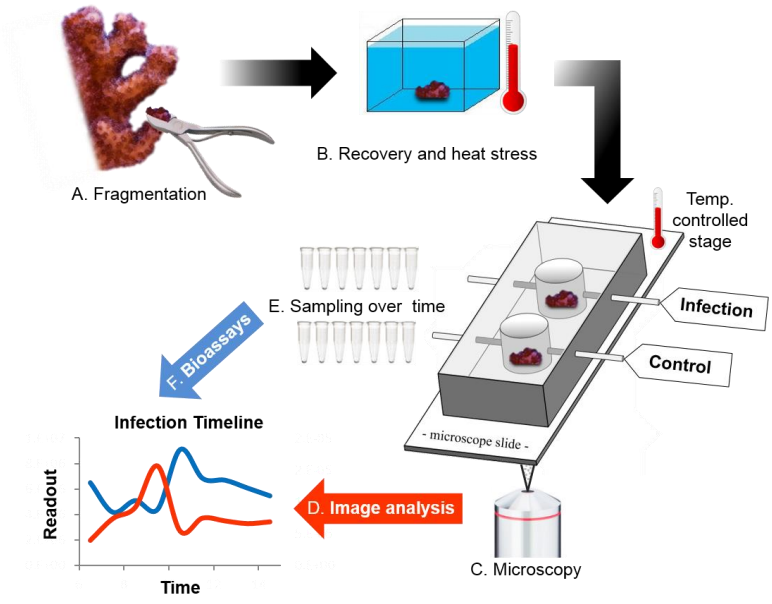

100

101 **Figure 1: Experimental work-flow for Microfluidic Coral Infection (MCI). A, B**. Small
102 coral fragments (~3-5 mm), clipped from the branch tips of a *P. damicornis* colony, are kept
103 in the main tank for recovery. Fragments are incubated for 3 days in a small (3.5 L)
104 temperature-controlled tank filled with filtered aquarium water. Heat stress is induced by
105 setting tank temperature to 30°C. **C**. Fragments are transferred to the MCI device placed on
106 a temperature-controlled microscope stage. Infection is initiated by introducing DsRed-
107 labelled *V. coralliilyticus* cells at desired duration and concentration through the inflow.
108 Infection progress is tracked using epifluorescence and light microscopy at set intervals. **D**.
109 Image analysis is used to quantify signal intensity and localization in all channels
110 throughout the infection period. **E**. An automated fraction collector is used to sample flow
111 through at set intervals throughout the experiment. Collected fractions are immediately
112 cooled to below 2°C, with or without addition of fixative, for subsequent analysis. **F**.
113 Collected fractions are analyzed by various bioassays, enabling correlation of microscopic
114 observations and downstream analysis.

115 During infection experiments, challenged coral fragments were inoculated with
116 either the bacterial pathogen *V. coralliilyticus* or the non-pathogenic *V. fischeri,* both
117 labeled by DsRed[24, 25] to facilitate imaging. Non-challenged fragments received
118 FASW throughout the experiment. Tissue integrity, coral behavior, and
119 zooxanthellae fluorescence and localization, as well as localization of labelled
120 bacteria in challenged fragments, were microscopically monitored throughout each
121 experiment (Figure 2).

122 No morphological or behavioral changes were observed in non-challenged control
123 fragments from all experiments (Fig. 2A; supplementary video 1). In fragments
124 challenged by *V. fischeri* (10^8 cells/ml), accumulation of DsRed-labelled bacteria was
125 observed in the polyp pharynx over the 1st hour of inoculation. This was followed by
126 moderate spewing of bacterial-laden mucus from all polyps (Fig 2B; supplementary
127 video 2). No other morphological or behavioral changes were observed.

128 A markedly different response was observed in fragments challenged by *V.*
129 *coralliilyticus* (10^8 cells/ml). A total of 39 fragments, derived from 6 coral colonies,
130 were challenged over the course of 18 separate experiments (Supplementary Table
131 1). Within 15 minutes of inoculation, polyp contraction was observed in all *V.*
132 *coralliilyticus*-challenged fragments. Pathogens accumulated in the coral pharynx
133 over the next hour, with little or no accumulation observed on other parts of the
134 coral surface (Figure 2C). Over the following 2-3 hours, polyps released copious
135 amounts of viscous, bacterial-laden mucus, concomitant with substantial stretching
136 of the coenosarc tissue connecting neighboring polyps (Figure 2C, Supplementary
137 Video 3, 4).

138 Following this stage, experiment results followed one of two outcomes (Figure 3). In
139 7 of the challenged experiments, consisting of 14 coral fragments, a complete or
140 near-complete recovery was observed (Supplementary Table 1). In these fragments
141 tissue confluence was retained, and within a few hours of inoculation polyps
142 expanded, with no labeled *V. coralliilyticus* cells observed in the pharynx
143 (Supplementary video 3).

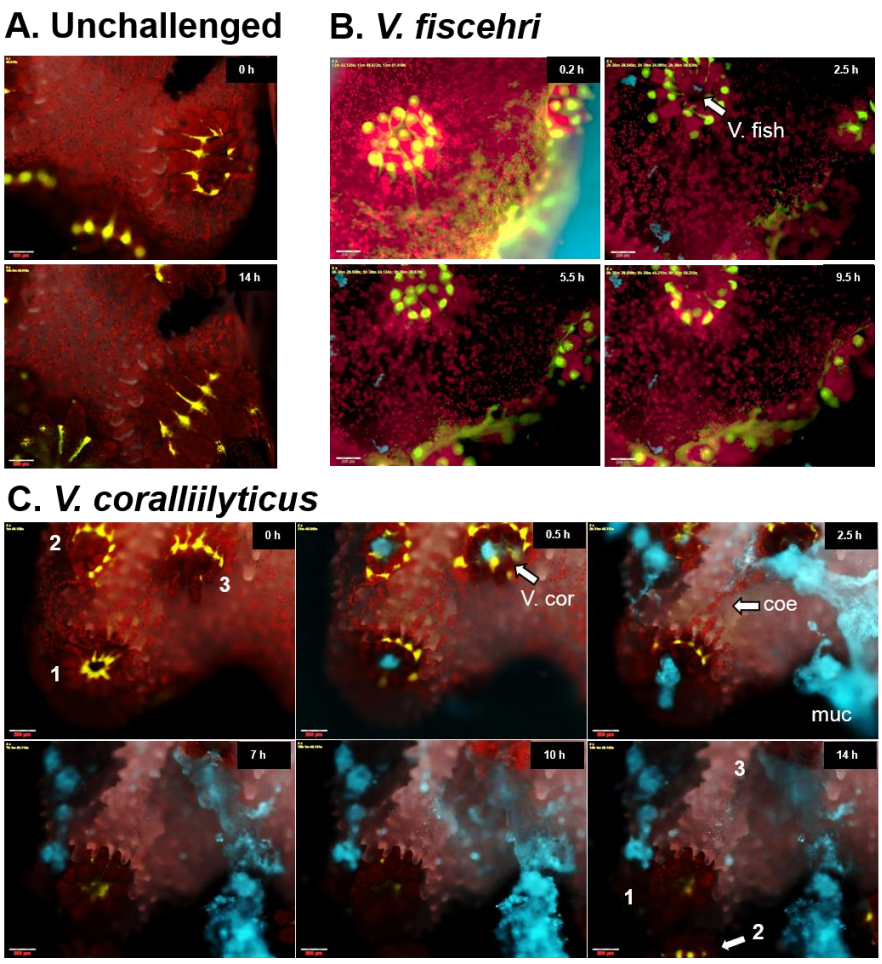

Figure 2: Timeline of a coral infection. A. Microscopic view of an unchallenged control *P. damicornis* fragment showing coral GFP (Green) and algal chlorophyll (Red). All non-challenged fragments appeared healthy at the end of the experiment (here 14 hours), with tentacles extended and no apparent bleaching or tissue loss. **B.** In *P. damicornis* fragments challenged by *V. fischeri*, slight accumulation of DsRed-labelled bacteria (cyan; V. fish) was observed in the coral pharynx. No disease-like symptoms were observed. **C.** Fragments challenged by *V. coralliilyticus* regularly displayed behavioral and morphological changes: Time **'0 h'**- Immediately prior to inoculation. Image shows three polyps (1-3) with partially extended tentacles. **0.5 h** – DsRed-labelled *V. coralliilyticus* (Cyan) accumulate at the polyp pharynx, but not on other exposed areas of the colony. **2.5 h** – Polyps secrete large amounts of mucus (muc), clearly visible due to large numbers of *V. coralliilyticus* cells adhering to it. Tearing of coenosarc tissue (coe) is observed. **7 h** –Coenosarc is degraded and polyps separated. Polyp **2** underwent polyp bail-out and is lost from the field of view. Polyp **3** is dead, with tissue degraded and GFP signal lost, although some chlorophyll autofluorescence is still observed. **10 h** - *V. coralliilyticus* accumulates on the exposed skeleton. **14 h** –At the end of the experiment polyp **1** remains viable, despite complete loss of surrounding tissue. A bailed-out polyp (possibly polyp **2**) is visible at the bottom of the image. Vacant calyx of polyp **3** is marked. Scale for all images are 200 µm.

Contrastingly, in the remaining 11 experiments, consisting of 25 challenged fragments, a clear pathology was observed (Figure 2C; Supplementary video 4). In these fragments, mucus spewing was followed by tearing of the coenosarc, leading to the separation of neighboring polyps and consequently loss of colony integrity (Fig. 2C). The majority of polyps in these experiments then underwent necrosis, manifested as visible loss of tissue integrity, accompanied by a gradual decay in GFP fluorescence (Figure 2C [Polyp 3]; Figure 4B; Supplementary figure 2). In 23 of these 25 fragments partial survival was observed in the form of polyp bail-out[24, 26]. In 4 of these 23 fragments, individual polyps survived and remained attached to the skeleton at the end of the experiment (Figure 2C; Figure 3; Supplementary Video 4; Supplementary Table 1).

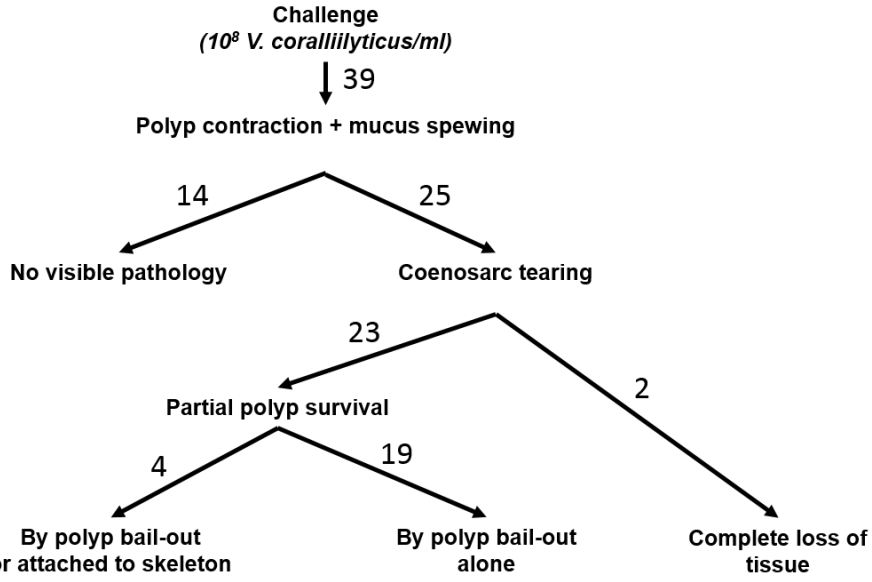

Figure 3. A roadmap of outcomes of for 39 *P. damicornis* fragments challenged by *V. coralliilyticus*. Polyp retraction and subsequent mucus spewing was observed in all fragments. In symptomatic fragments, this was followed by separation of neighboring polyps through coenosarc tearing. Individual polyps underwent one of three different fates (survival, bail-out or death).

Lesion infection

A slightly modified infection sequence was observed in fragments with minor lesions in the coenosarc tissues. *V. coralliilyticus* cells regularly accumulated at the lesion edge (Figure 4; Supplementary Video 5) within the first hour of inoculation. Further bacterial accumulation or proliferation was observed over the next hours, accompanied by tissue necrosis manifested as rapid tearing or degradation of the ceonosarc tissue and death of neighboring polyps.

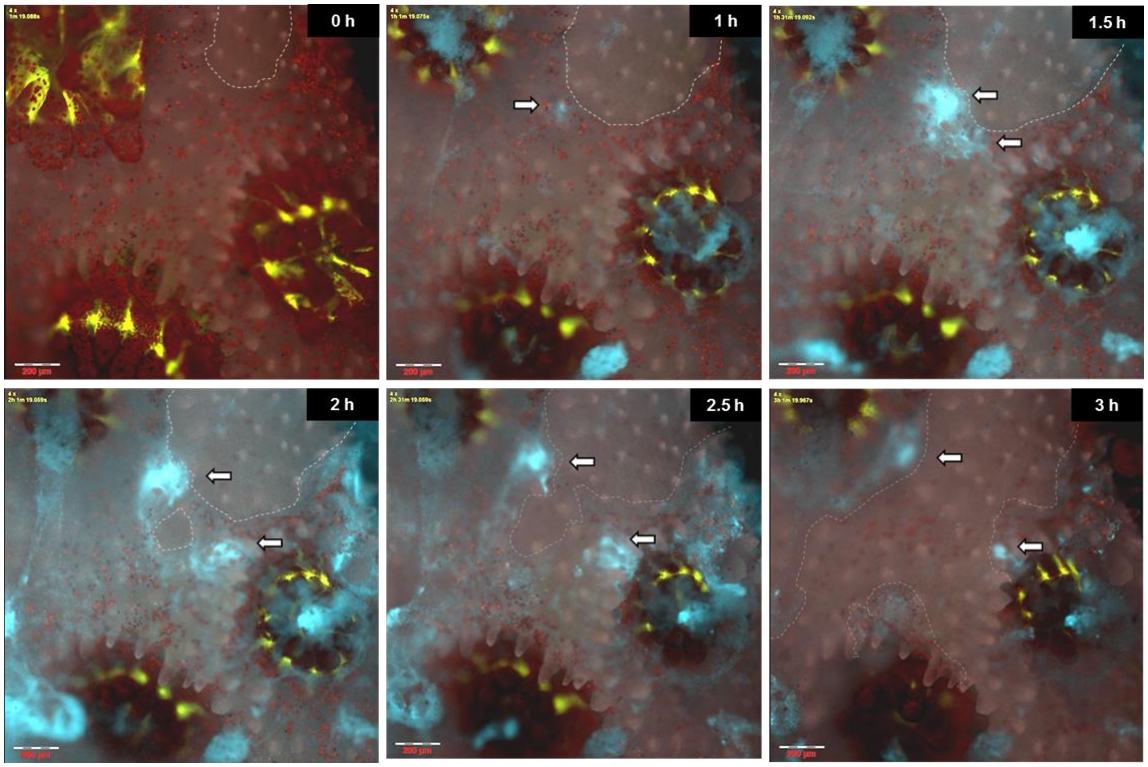

Figure 4: Tissue lesions allow rapid colonization and infection. Time **'0' h** – Infected fragmented immediately prior to inoculation. Coral GFP (Green) and algal chlorophyll (Red) are shown on a greyscale background. Dashed line marks the borders of a small lesion approximately 300 µm in diameter. **1 h** – *V. coralliilyticus* cells (Cyan) accumulate at the lesion edge (arrow). **1.5 h – 3 h** – further colonization of the torn tissue is followed by rapid lesion expansion and death of neighboring polyps. The complete sequence from this experiment is provided in supplementary video 4. Scale bars are 200 µm**.**

Quantitative image analysis

Quantification of fluorescence intensity derived from the different components of the holobiont (GFP for coral tissue, chlorophyll for algal symbionts and DsRed for *V. coralliilyticus*) provided further information on the infection progression in challenged fragments (Figure 5A, B). A gradual but constant decrease in coral GFP intensity, beginning approximately 2 h post inoculation, was consistently observed in dying fragments, but not in non-challenged controls or in challenged, asymptomatic fragments (Figure 5A, B). The most prominent feature in the resulting DsRed intensity profile was a large peak spanning the first 2 hours of each experiment, reflecting the inflow of labeled *V. coralliilyticus* during inoculation (Figure 4B). A smaller peak in the DsRed channel regularly appeared between 6 and 10 hours following inoculation. No distinct patterns were observed in chlorophyll autofluorescence within the timeframe of the infections described here.

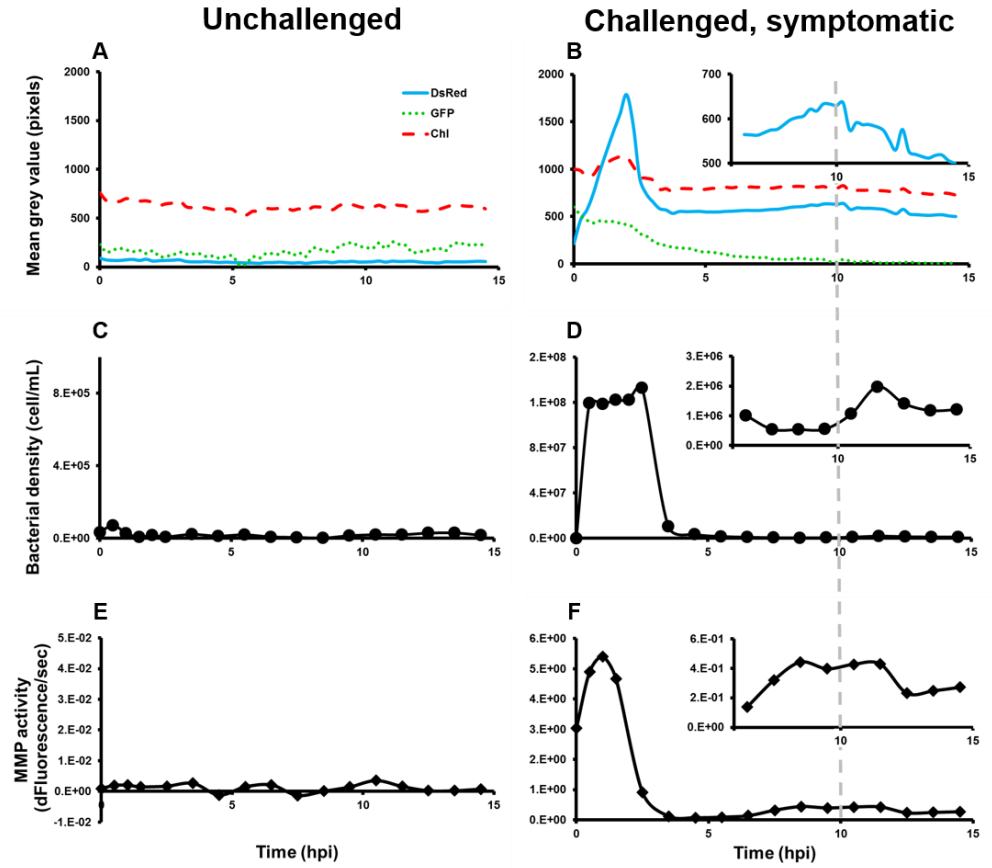

Figure 5: Quantitative analysis of microscope images and system exudates provide further insights into the timeline of coral infection. A, B – Quantification of fluorescence signals from GFP (green), Chlorophyll (red) and DsRed labeled *V. coralliilyticus* (cyan) in unchallenged (**A**) and challenged by *V. coralliilyticus* (**B**) fragments. High levels of DsRed signal over the first 2 hours of experiment in **B** correspond to pathogen inoculation and settlement of the coral pharynx. A gradual decrease in GFP signal starting approximately 2 hours post-infection indicates death and disintegration of the coral host. The increase in DsRed signal between 6 and 10 h (**B**, inset) likely indicates pathogen proliferation at the expense of the dying coral. **C, D**. Quantification of total bacterial density in the outflow of a control (**C**) and infected (**D**) chambers. High bacterial load in **D** over the first 2 hours indicate relatively low attachment of inoculated *V. coralliilyticus* to the coral host. A slight increase in bacterial density starting at 10 h (**D**, inset), termed "late burst", is likely driven by pathogens, and possibly other bacteria, released from the dying tissue. **E, F**. Quantification of matrix metalloproteinases (MMPs) activity in the outflow of a control (**E**) and infected (**F**) chambers. Initial high activity corresponds to MMPs activity in the inoculum. Increased activity starting at 7 hours (**F**, inset) may indicate increased MMPs production by *V. coralliilyticus* as it breaks down the host tissue.

Downstream microbial and biochemical analysis of MCI exudates

Additional insight into the infection process was gained by time-resolved measurement of microbial abundance and MMP activity in the MCI exudates (Figure 5C-F; Supplementary figures 3, 4). The highest values for both MMP activity and cell abundance were measured during the initial two-hour inoculation period. In all challenged fragments, bacterial abundance in the exudates decreased following inoculation from 10^8 cells/mL to approximately 10^6 cells/mL (Figure 5D; Supplementary figures 3A, 4A), with a corresponding decrease in MMP activity (Fig. 5F; Supplementary figure 3B, 4B). In challenged, symptomatic fragments a subsequent rise of up to 10 fold in MMP activity was regularly observed starting at 4-6 h post inoculation (Fig. 5F; Figure 6; Supplementary figure 4B). This increase was followed by an increase in bacterial load of up to half an order of magnitude at 7-10 hours post inoculation (Figure 5D; Supplementary figure 4A). These late increase in bacterial abundance and MMP activity were not observed in either the challenged, non-symptomatic fragments or in fragments challenged with *V. fischeri.* Comparing total and DsRed-labeled bacterial numbers in the outflow of one

243 experiment revealed that the portion of DsRed labelled bacterial cells went down
244 from 100% labeling in the inoculum to 70-90% in the following 8h, and further
245 decrease to 60% during the subsequent rise in bacterial abundance starting at 9.5 h
246 from inoculation (Supplementary Figure 5).

247 By integrating the various measurement and observations from all MCI experiments
248 into a single timeline we were able to generate the most detailed description to-date
249 of the infection of a reef building coral by a bacterial pathogen (Fig. 6). This unified
250 timeline reveals the conservation of the different stages described here, as well as
251 some variability in the relative timing of specific events, particularly in the later
252 stages. From this integrated timeline it is evident that initial polyp contraction and
253 mucus spewing was an immediate response shared by all fragments regardless of
254 their ultimate fate. The rise in MMP activity was always preceded by the onset of
255 tissue lysis, and was generally preceded by GFP decay. The rise in bacterial
256 abundance in the effluent was generally observed following the rise in MMP activity.
257 In the majority of actively infected fragments, the entire infection process was
258 complete within 10-15 hours following inoculation.

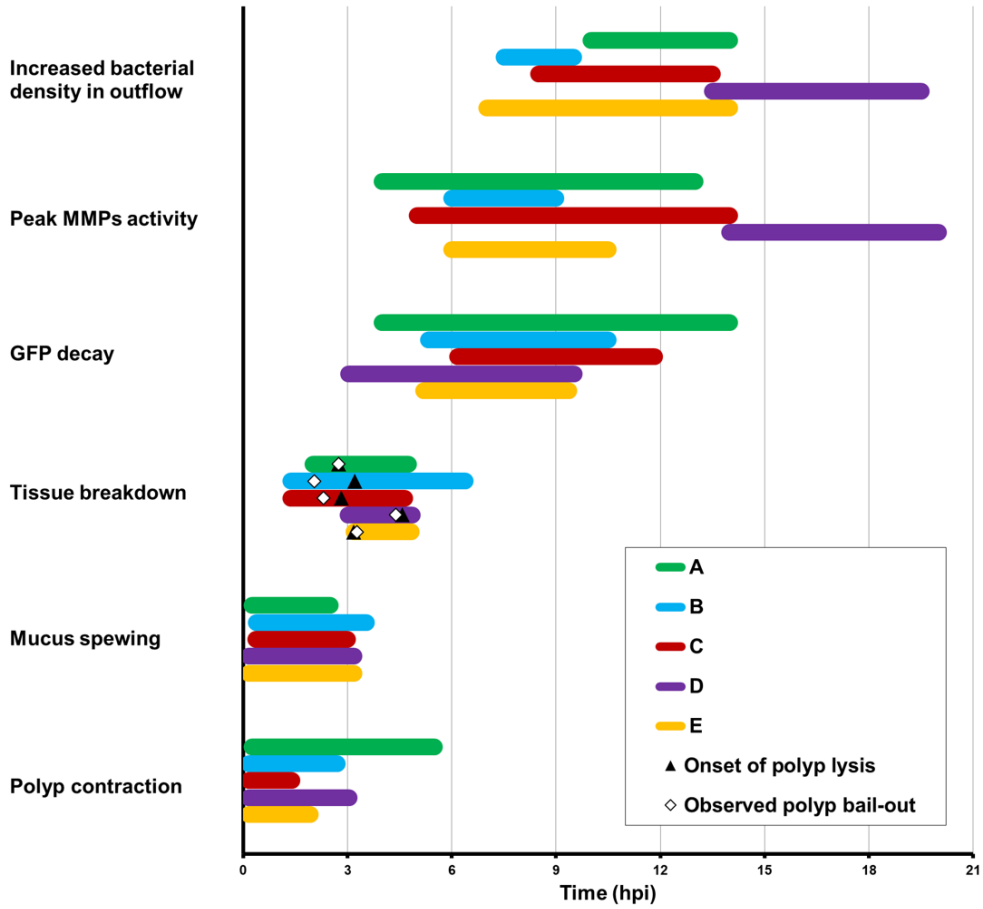

259

260 **Figure 6: Summary of key infection phases.** Results from 5 representative experiments
261 using fragments from three *P. damicornis* colonies (A-E; see details in Supplementary Table
262 1). Only fragments showing clear symptoms following challenge by *V. coralliilyticus* are
263 represented. The overall sequence of morphological, biochemical and microbial events is
264 highly conserved although exact timing of events varied. Colored bars represent approximate
265 duration of observation or measurement for each experiment. Discrete observations related
266 to colony breakdown, including polyp bail-out and tissue lysis, are marked on the
267 corresponding bar as (◊) and (▲), respectively.

Discussion

Coral disease progression is often studied at scales ranging from single colonies to the entire reef, thus overlooking the microscale processes governing host-pathogen interactions. While important insights into disease etiology have been gained by careful pathological and histological studies [23, 27-30], such studies are mostly limited to snapshots of the disease process at acute and morphologically recognizable phases[8, 13, 31-33]. Thus, an *in vivo* description of the sequence of microscopic events underlying the process of coral infection is still missing. The current work aims to bridge this gap, by studying coral disease under controlled laboratory conditions, at temporal and spatial scales relevant to the microscopic interactions between a bacterial pathogen and its coral host.

Using live-imaging microscopy we are able, for the first time, to visualize *V. coralliilyticus* as it colonizes and infects its coral host. Rather than colonizing the entire colony surface, we show that bacterial accumulation occurs primarily at the polyp pharynx, which points towards a gastrovascular route of infection. This is in agreement with observations reported in our previous work, demonstrating accumulation of *V. coralliilyticus* in the gastrovascular cavity of micropropagated *P. damicornis* polyps[24]. Following inoculation the majority of coral fragments displayed a clear pathology leading to colony disintegration followed by the release of *V. coralliilyticus* cells to the surrounding water. Accumulation at the coral pharynx was also observed in coral fragments challenged with *V. fischeri*, but to a lesser extent and no apparent pathology. Colonization of the colony surface in our experiments appeared to be limited to sites of tissue lesions, which may serve as hotspots of bacterial infection.

Beyond tracking of the bacterial pathogen, the MCI provides us with the unique ability to observe microscale patterns of coral behavior, a subject that is rarely considered in the context of coral disease. We were thus able to describe and characterize the sequence of behavioral responses of the coral host following a bacterial challenge. We observed specific coral reactions immediately following

297 inoculation with pathogenic *V. coralliilyticus,* particularly the retraction of coral
298 polyps into their calices followed by mucus spewing, that were distinct from those
299 observed following a challenge by the non-pathogenic *V. fischeri*. Polyp retraction is
300 a universal response of corals to physical or environmental stress[34], indicating that
301 the coral is sensing, and responding to, the presence of pathogens or their exudates.
302 Moreover, as polyp retraction minimizes intake of water into the polyp
303 gastrovascular system, and thus the internalization of planktonic food[35-37], this
304 behavior may also provide a means for the coral to avoid further accumulation of
305 pathogens in its gastric cavity. The subsequent spewing of viscous, bacterial-laden
306 mucus from the polyp mouth may be interpreted as further attempt by the coral to
307 rid itself of the ingested pathogens, not unlike the coughing of phlegm during a
308 throat or lung infection. Again, mucus spewing is a common coral response to high
309 loads of food or particulate matter in surrounding water[38-40]. However, considerably
310 less mucus was secreted in response to challenge with *V. fischeri,* suggesting that
311 coral challenged by *V. coralliilyticus* experience stress that is not directly related to
312 the presence of bacterial cells in the surrounding water. Thus, polyp contraction and
313 mucus spewing may be considered an important coral defense behavior when faced
314 with high loads of bacterial pathogens in their environment.

315 In all *V. coralliilyticus*-challenged fragments, mucus spewing was invariably followed
316 by stretching of ceonosarc tissues. In symptomatic fragments, this ultimately led to
317 tearing of the tissue and separation of adjacent polyps. Surprisingly, many of these
318 isolated polyps survived, some remaining attached to the skeleton while most
319 undergoing polyp bail-out[24, 26]. Notably, bailed out polyps collected and maintained
320 in filtered sea-water following infection experiments remained viable for over two
321 weeks, suggesting that these polyps were indeed able to overcome the invading
322 pathogen. Polyp separation thus provides the coral with an additional defense layer,
323 enabling it to quarantine disease by "sacrificing" infected polyps. This response
324 likely prevents pathogens from spreading to the rest of the colony through the
325 common gastrovascular system, similar to plant hypersensitive resposne[41]. Polyp
326 bail-out may further promote the survival of the genotype by salvaging individual

polyps from doomed colonies, which may settle and regenerate into new colonies where conditions are more favorable[24, 26, 42].

A major question arising from our results relates to the function of matrix metaloproteases (MMP) in the infection sequence. MMPs were previously suggested to be a key virulence factor of *V. coralliilyticus*[18]. In our experiments, despite the exposure of all treated corals to unnaturally high levels of MMPs secreted by the bacterial pathogens during inoculation step (Figure 5B), over 30% of the corals ultimately survived the infection. Thus, under the conditions tested, MMP activity alone was not sufficient to kill the corals. This is in agreement with previous work reporting similar infectivity of a different strain of *V. coralliilyticus* following deletion of a gene encoding MMP production[12]. In our experiments we observe a rise in MMP activity at a relatively late stage of the infection, when polyps are likely already dead or dying as indicated by the decay in GFP signal. The secretion of metaloenzymes at this stage suggests their involvement in the breakdown of coral tissue, as a means for *V. coralliilyticus* to scavenge nutrients and essential metabolites from the dying colony.

An interesting observation arising from our experiments was that a large fraction of the microorganisms released in the system's exudates over the course of the infection were not DsRed-labeled (Supplementary figure 5). While this may be explained by the loss of DsRed-encoding plasmids from transformed *V. coralliilyticus*, an alternative explanation is that additional bacterial populations, formerly part of the coral holobiont, benefit from the lysis of the coral tissue and the associated abundance of nutrients. Future analysis of the bacterial community released from corals infected under similar settings may provide further insights into the identity and nature of such rogue members of the coral microbiome.

One of our goals in constructing the MCI system was to elucidate the route of infection and disease initiation. Previous studies demonstrated involvement of motility in pathogenic *Vibrio*-coral interactions, and suggested that chemotaxis towards coral mucus facilitates host-localization and colonization of the coral

356 surface[43-46]. This view is challenged by a recent work demonstrating increased
357 infectivity of *V. coraliilyticus* cells with impaired chemotaxis[47], similar to results in *V.*
358 *cholera*[48] but differing from the fish pathgoen *V. anguillarum*[49]. Indeed, bacterial
359 chemotaxis occurs over relatively short distances (100's of microns) and requires a
360 stable and continuous gradient of the chemoattractant[50]. As recently demonstrated,
361 such conditions are not typically found near the surface of scleractinain corals.
362 Ciliary flows exceeding 1 mm/s at the coral surface actively mix the coral's bounday
363 layer by creating vortices extending up to 2 mm into the surounding water[51]. These
364 rapid currents, ten time the swimming speed of *V. coralliilyticus*[17], disrupt diffusion
365 gradients that would otherwise develop in the coral's boundary layer, while
366 sweeping away any pathogens reaching the coral's surface. Thus, ciliary flows are
367 likely to prevent pathogens of scleractinian corals from chemotaxing towards their
368 potential hosts.

369 This putative role of cilia as a physical barier to bacterial colonization is further
370 supported by the observed accumulation of pathogens at tissue lesions, where
371 tissue confluence is breached and ciliary motion is likely disrupted. Such local
372 patches of reduced ciliary flow, possibly enriched with infochemicals exuded from
373 the torn tissue, may indeed facilitate bacterial chemotaxis. This may account for the
374 rapid colonization and infection at lesion sites in our experiments. Indeed, previous
375 studies showed that wounds caused by trauma to coral colonies provide "hot spots"
376 for initiation of various coral diseases, including white plague, brown and black
377 band, and others[52-54]. Here we show that even minor lesions, under the right
378 conditions, may serve as a possible point of entry for bacterial pathogens.

379 The question of chemotaxis is also relevant to the accumulation of pathogens at the
380 coral pharynx. Significantly, while pathogen accumulation at lesion sites was only
381 observed 45-60 minutes from inoculation, comparable accumulation at the coral
382 pharynx is observed already 10-15 minutes into the experiment, suggesting
383 different mechanism may be driving the two phenomena. We suggest that
384 accumulation at the pharynx may be driven by the active uptake of water into the
385 coral's gastrovascular system prior to polyp contraction, as part of ongoing feeding

386 and gas exchange processes[37, 55-57]. Once inside the gastrovascular channels, where
387 flow is likely to be laminar and boundaries within easy reach, chemotaxis may well
388 play a part in bacterial colonization of the gastrovascular mucus.

389 The use of small coral fragments in our system allowed us to perform a relatively
390 large number of experiments, using fragments from multiple colonies. An
391 unexpected result was the heterogeneity in the response of different *P. damicornis*
392 colonies to *V. coralliilyticus* infection (Supplementary Table 1). While some colonies
393 were highly susceptible to infection (e.g. colonies 2 and 5), other colonies had
394 remarkably high survival rates (e.g. colonies 3 and 4). The mechanisms underlying
395 these differences are not clear. Genetic differences, life histories or microbiome
396 composition may all contribute to coral resilience[58-62]. Heterogeneity was also
397 observed at the response of individual polyps, and that too requires further
398 investigation. Future experiments examining the genetic and epigenetic (including
399 microbiome composition) background of different colonies may help resolve some
400 of these questions.

401 It is important to note that in all bacterial challenge experiments reported here, we
402 used approximately 10^8 *V. coralliilyticus* cells/ml, a number that is clearly unrealistic
403 ecologically. Inoculations with 10^7 cells/ml or less did not result in coral mortality
404 under the conditions tested, even following 72 hours of subsequent incubation (data
405 not shown). While this may signify a limitation of the short duration of our
406 experiments, it is notable that previous experiments reported for the same coral-
407 pathogen system also used *V. coralliilyticus* concentrations of between 10^7 and 10^8
408 cells/ml to induce infection[9, 14, 46]. Ushijima and colleagues[47] determined the
409 infectious dose of *V. coralliilyticus* towards *Montipora* to be between 10^7 and 10^8
410 cells/ml. This suggests a compatible coral immunity and high resilience to the low
411 densities of planktonic *V. coralliilyticus* prevalent in the reef environment[63]. An
412 alternative route for coral infection under natural conditions, which remains to be
413 explored, is the ingestion of vibrio-laden marine snow or infected zooplankton,
414 delivering an infective dose of bacterial pathogens directly into the corals'
415 gastrovascular system[64].

The MCI experimental setup, presented here for the first time, combines advanced live imaging microscopy, microfluidics and time resolved sampling and analysis of the system effluents enabling the evaluation of coral-pathogen interactions at unprecedented detail. This revealed several hitherto unknown aspects of coral disease, including localization of pathogens at the onset of infection, behavioral defensive responses of the coral host, and the heterogeneity of polyp fate following infection, and defined distinct phases of the infection process. Future application of approaches similar to that described here will facilitate more detailed understanding of the complex and ecologically important interactions occurring between corals and their bacterial pathogens. This platform will provide a foundation for future studies aiming at elucidating the versatile adaptive response of the fragile coral ecosystems to fluctuating environments.

Methods

MCI experimental setup

Microfluidic chambers were fabricated *in-house* as follows: A 5x1.5 cm slab was cut out of a 5 mm thick sheet of polydimethylsiloxane (PDMS) silicone elastomer (Sylgard® 184) using a utility knife. 4-6 Ø8mm wells were punched into the resulting slab using a biopsy punch of the same diameter, forming chambers of approximately 250µL. Inlet and outlet holes were punched into opposing sides of each chamber using a 1 mm biopsy punch (Integra®, Fischer Scientific). (Supplementary figure 1). The PDMS slab was then bonded to a glass microscope slide by exposing both to oxygen plasma for one minute using a laboratory Corona Treater (Electro-Technic Products). Each chamber was fitted with polyethylene inlet and outlet tubing (BPE-60, Instech Laboratories) (Fig 1). The assembled device was placed on a temperature controlled microscope stage. Small *P. damicornis* fragments (3-5 mm) were placed in each chamber and chambers sealed with ApopTag® Plastic cover slips (Merck). Flow (2.6 mL $hour^{-1}$) was generated using a peristaltic pump (Ismatec) connected to the outlet tube. The input tube was connected to a flask

444 containing FASW (0.22 μm). Inoculation was carried out by transferring the free end
445 of the inlet tube to a flask containing FASW supplemented with 10^8 of either *V.*
446 *coralliilyticus* or *V. fischeri* for 2 h, and then transferring back to the FASW-
447 containing flask.

448 The outlet stream from each chamber was continuously collected using a 4 channel
449 fraction collector (Gilson Inc.) into 2 ml Eppendorf tubes, with tubes for each stream
450 changed at 30 min intervals. Tubes were maintained in an aluminum tube rack
451 placed in an ice bath to maintain contents at 0-1°C. Every 2nd tube was
452 supplemented in advance with paraformaldehyde (PFA) to a final concentration of
453 approximately 1%, enabling subsequent bacterial quantification using flow
454 cytometry. Fractions from tubes without fixative were centrifuged, and supernatant
455 used for quantification of MMP enzymatic activity.

456 **Coral collection and handling.**

457 All *P. damicornis* colonies used in this study were collected from a coral nursery
458 located at a depth of 8 m off the pier of the Inter-University Institute, Eilat, Israel
459 (Israel nature and parks authority permit No # 2014/40327). Collected corals were
460 maintained in an aquarium at the Weizmann Institute of Science. Small branch tips
461 were clipped from the colonies and left in the main tank for recovery for at least one
462 week. Prior to each experiment some fragments were transferred to a separate 4 L
463 tank filled with FASW and incubated at 31◦C for a period of 3 days. The fragments
464 were then transferred to the MCI device for microscopic observation. At the
465 beginning of each experiment, prior to inoculation, fragments were acclimated on
466 the stage for at least 3 hours with a constant flow of filtered aquarium water.

467 ## *Vibrio coralliilyticus* transformation to express DsRed

468 Infection experiments were performed using the *V. coralliilyticus* strain YB2 labelled
469 with a plasmid encoding for a potent variant of DsRed2 fluorescent protein[25] as
470 described previously[24]. For each experiment, DsRed-labelled *V. coralliilyticus* were
471 grown overnight from glycerol stock at 30 °C in Zobell Marine Broth. Bacteria were

then centrifuged (3500 G, 5 minutes) and resuspended in FASW. Tubes were then incubated at 30˚C with no shaking to allow sinking of non-motile bacteria.

Infection assays procedure

Experimental procedure

The general work flow and infection scheme is illustrated in **Error! Reference source not found.**. Inoculation was carried out by flowing a suspension of DsRed-labeled *V. coralliilyticus* or *V, fischeri* (approximately 10^8 cells/mL) into the chamber over a period of two hours. Inlet flow was then switched to filtered aquarium water for the remaining incubation. Live imaging microscopy was carried out using a fully motorized inverted fluorescence microscope (Olympus IX81) equipped with a Coolsnap HQ2 CCD camera (Photometrics). Throughout the infection experiments, multichannel micrographs of the fragments were captured every 15 minutes at 4X magnification. This enabled visualization of the coral-tissue GFP, zooxanthellae chlorophyll, and DsRed fluorescence, alongside a bright-field channel.

Image analysis

Image analysis was carried out using imageJ (FIJI), by measuring mean grey intensity (in pixels) of the entire frame in each channel (GFP, Chlorophyl, and DsRed) captured at every time point.

Downstream exudate analysis

To couple the visual observations with direct microbial and biochemical measurements, each chamber's effluents was continuously collected in a time resolved manner using a fraction collector and immediately cooled to between 0 and 2°C (Figure 1, step 5). Odd numbered fractions (1.3 mL) each were immediately fixed in 1% PFA in FASW. 20 µL of each sample was diluted 10 fold and stained with nucleic acid stain SYBR-gold (Invitrogen). Cell abundance was measured using a flow cytometer (iCyt Eclipse, excitation: 488 nm, emission: 500–550 nm). Even numbered fractions were collected with no fixation and filtered through 0.22 µm

499 syringe filter (Millipore). Filtrate was used to estimate MMP activity using a specific
500 fluorescent substrate (Calbiochem MMP-2/MMP-7 Substrate, Fluorogenic) in a
501 microplate reader (Tecan Infinite® M200pro). Fluorescence (exitation :325 nm,
502 emmition: 393 nm) was measure every 90 seconds at 30°C for 40 min. We used a
503 specific MMPs substrate to demonstrate that isolated *V. coralliilyticus* secretes
504 MMPs to the culture medium during different growth phases (Supplementary figure
505 6A). This specific activity was confirmed by inhibition with GM6001, a broad-
506 spectrum MMPs inhibitor with inhibition capacity of IC_{50} = 5 µM (Supplementary
507 figure 6B).

508

509 **Author contributions**

510 ARG and OHS developed the MCI experimental setup. ARG transformed *V.*
511 *coralliilyticus* and performed the experiments and image analysis. EKW contributed
512 to experimental design and interpretation of results. AV contributed to the design
513 and evaluation of the experiments and the overview of all aspects of the project.
514 ARG, OHS, EKW, and AV wrote the manuscript.

515 **Acknowledgements**

516 *V. coralliilyticus* transformation was carried out with the help of D. Schatz using
517 materials and protocols generously provided by Prof. E. Stabb (Franklin College,
518 University of Georgia). Inna Solomonov and Irit from the Irit Sagee lab, Weizmann
519 Institute of Science, are assisted with establishment and validation of the MMP
520 activity essay. This work was supported by the Human Frontiers in Science Program
521 (award #RGY0089), the Weizmann - EPFL Collaboration Program (grant number:
522 721236), and the Angel Faivovich Foundation for Ecological research.

References

1. Hoegh-Guldberg, O. & Bruno, J. F. The impact of climate change on the world's marine ecosystems. *Science* **328**, 1523-1528 (2010).

2. Rosenberg, E., Kellogg, C. A. & Rohwer, F. L. Coral microbiology. *OCEANOGRAPHY-WASHINGTON DC-OCEANOGRAPHY SOCIETY-* **20**, 146 (2007).

3. Rohwer, F., Youle, M. & Vosten, D. in *Coral reefs in the microbial seas* (Plaid Press, 2010).

4. Haas, A. F. *et al*. Global microbialization of coral reefs. *Nature microbiology* **1**, 16042 (2016).

5. Roth, E., Jeon, K. & Stacey, G. Homology in endosymbiotic systems: The term'symbiosome'. (1988).

6. Zvuloni, A. *et al*. Spatio-temporal transmission patterns of black-band disease in a coral community. *PLoS One* **4**, e4993 (2009).

7. Peters, E. C. in *Coral Reefs in the Anthropocene* 147-178 (Springer, 2015).

8. Kushmaro, A., Rosenberg, E., Fine, M., Ben Haim, Y. & Loya, Y. Effect of temperature on bleaching of the coral Oculina patagonica by Vibrio AK-1. *Mar. Ecol. Prog. Ser.* **171**, 131-137 (1998).

9. Ben-Haim, Y. *et al*. *Vibrio coralliilyticus sp. nov*., a temperature-dependent pathogen of the coral Pocillopora damicornis. *Int. J. Syst. Evol. Microbiol.* **53**, 309-315 (2003).

10. Rosenberg, E., Kushmaro, A., Kramarsky-Winter, E., Banin, E. & Yossi, L. The role of microorganisms in coral bleaching. *The ISME journal* **3**, 139-146 (2009).

11. Kramarsky-Winter, E., Downs, C., Downs, A. & Loya, Y. Cellular responses in the coral Stylophora pistillata exposed to eutrophication from fish mariculture. *Evol. Ecol. Res.* **11**, 381-401 (2009).

12. Santos, E. *et al*. Genomic and proteomic analyses of the coral pathogen *Vibrio coralliilyticus* reveal a diverse virulence repertoire. *The ISME journal* **5**, 1471-1483 (2011).

13. Y., B. & E., R. A novel Vibrio sp. pathogen of the coral Pocillopora damicornis. *Mar. Biol.* **141** (2002).

14. Vidal-Dupiol, J. *et al*. Coral bleaching under thermal stress: putative involvement of host/symbiont recognition mechanisms. *BMC physiology* **9** (2009).

554 15. Zvuloni, A., Artzy-Randrup, Y., Katriel, G., Loya, Y. & Stone, L. Modeling the impact
555 of white-plague coral disease in climate change scenarios. *PLoS computational biology*
556 **11**, e1004151 (2015).

557 16. Wright, R. M. *et al*. Intraspecific differences in molecular stress responses and
558 coral pathobiome contribute to mortality under bacterial challenge in Acropora
559 millepora. *Sci. Rep.* **7**, 2609-017-02685-1 (2017).

560 17. Garren, M., Son, K., Tout, J., Seymour, J. R. & Stocker, R. Temperature-induced
561 behavioral switches in a bacterial coral pathogen. *The ISME journal* **10**, 1363-1372
562 (2016).

563 18. Sussman, M. *et al*. Vibrio zinc-metalloprotease causes photoinactivation of coral
564 endosymbionts and coral tissue lesions. *PLoS One* **4**, e4511 (2009).

565 19. Rosenberg, E. & Kushmaro, A. in *Coral Reefs: An Ecosystem in Transition* 451-464
566 (Springer, 2011).

567 20. Bourne, D. *et al*. Microbial disease and the coral holobiont. *Trends Microbiol.* **17**,
568 554-562 (2009).

569 21. Pollock, F. J., Morris, P. J., Willis, B. L. & Bourne, D. G. The Urgent Need for Robust
570 Coral Disease Diagnostics. *PLoS Pathog* **7**, e1002183 (2011).

571 22. Weis, V., Davy, S., Hoegh-Guldberg, O., Rodriguez-Lanetty, M. & Pringle, J. Cell
572 biology in model systems as the key to understanding corals. *Trends in ecology &*
573 *evolution* **23**, 369-376 (2008).

574 23. Work, T. & Meteyer, C. To Understand Coral Disease, Look at Coral Cells.
575 *EcoHealth*, 1-9 (2014).

576 24. Shapiro, O. H., Kramarsky-Winter, E., Gavish, A. R., Stocker, R. & Vardi, A. A coral-
577 on-a-chip microfluidic platform enabling live-imaging microscopy of reef-building
578 corals. *Nature communications* **7**, 10860 (2016).

579 25. Dunn, A. K., Millikan, D. S., Adin, D. M., Bose, J. L. & Stabb, E. V. New rfp- and pES213-
580 derived tools for analyzing symbiotic *Vibrio fischeri* reveal patterns of infection and
581 lux expression in situ. *Appl. Environ. Microbiol.* **72**, 802-810 (2006).

582 26. Sammarco, P. W. Polyp bail-out: an escape response to environmental stress and
583 a new means of reproduction in corals. *Marine ecology progress series.Oldendorf* **10**,
584 57-65 (1982).

585 27. Work, T. M. & Aeby, G. S. Pathology of tissue loss (white syndrome) in Acropora
586 sp. corals from the Central Pacific. *J. Invertebr. Pathol.* **107**, 127-131 (2011).

587 28. Work, T. M. & Aeby, G. S. Systematically describing gross lesions in corals. *Dis.*
588 *Aquat. Org.* **70**, 155-160 (2006).

589 29. Ainsworth, T., Fine, M., Roff, G. & Hoegh-Guldberg, O. Bacteria are not the primary
590 cause of bleaching in the Mediterranean coral Oculina patagonica. *The ISME journal*
591 **2**, 67 (2008).

592 30. Ainsworth, T. D., Fine, M., Blackall, L. L. & Hoegh-Guldberg, O. Fluorescence in situ
593 hybridization and spectral imaging of coral-associated bacterial communities. *Appl.*
594 *Environ. Microbiol.* **72**, 3016-3020 (2006).

595 31. Boyett, H. V., Bourne, D. G. & Willis, B. L. Elevated temperature and light enhance
596 progression and spread of black band disease on staghorn corals of the Great Barrier
597 Reef. *Mar. Biol.* **151**, 1711-1720 (2007).

598 32. Gignoux-Wolfsohn, S., Marks, C. J. & Vollmer, S. V. White Band Disease
599 transmission in the threatened coral, Acropora cervicornis. *Scientific reports* **2**, 804
600 (2012).

601 33. Kaczmarsky, L. T. Coral disease dynamics in the central Philippines. *Dis. Aquat.*
602 *Org.* **69**, 9-21 (2006).

603 34. Horridge, G. A. The co-ordination of the protective retraction of coral polyps.
604 *Philosophical Transactions of the Royal Society of London B: Biological Sciences* **240**,
605 495-528 (1957).

606 35. Levy, O., Dubinsky, Z., Achituv, Y. & Erez, J. Diurnal polyp expansion behavior in
607 stony corals may enhance carbon availability for symbionts photosynthesis. *J. Exp.*
608 *Mar. Biol. Ecol.* **333** (2006).

609 36. Gladfelter, E. Circulation of fluids in the gastrovascular system of the reef coral
610 Acropora cervicornis. (1983).

611 37. Patterson, M. R. A chemical engineering view of cnidarian symbioses. *Am. Zool.* **32**,
612 566-582 (1992).

613 38. Lewis, J. & Price, W. Feeding mechanisms and feeding strategies of Atlantic reef
614 corals. *J. Zool.* **176**, 527-544 (1975).

615 39. Brown, B. E. & Bythell, J. C. Perspectives on mucus secretion in reef corals. *Marine*
616 *Ecology Progress Series* **296**, 291-309 (2005).

617 40. Zetsche, E., Baussant, T., Meysman, F. J. & van Oevelen, D. Direct visualization of
618 mucus production by the cold-water coral Lophelia pertusa with digital holographic
619 microscopy. *PloS one* **11**, e0146766 (2016).

620 41. Lam, E., Kato, N. & Lawton, M. Programmed cell death, mitochondria and the plant
621 hypersensitive response. *Nature* **411**, 848-853 (2001).

622 42. Kvitt, H. *et al*. Breakdown of coral colonial form under reduced pH conditions is
623 initiated in polyps and mediated through apoptosis. *Proc. Natl. Acad. Sci. U. S. A.* **112**,
624 2082-2086 (2015).

625 43. Garren, M. *et al*. A bacterial pathogen uses dimethylsulfoniopropionate as a cue to
626 target heat-stressed corals. *The ISME journal* **8**, 999-1007 (2014).

627 44. Garren, M. & Azam, F. Corals shed bacteria as a potential mechanism of resilience
628 to organic matter enrichment. *ISME J.* **6**, 1159-1165 (2012).

629 45. Banin, E., Israely, T., Fine, M., Loya, Y. & Rosenberg, E. Role of endosymbiotic
630 zooxanthellae and coral mucus in the adhesion of the coral-bleaching pathogen Vibrio
631 shiloi to its host. *FEMS Microbiol. Lett.* **199**, 33-37 (2001).

632 46. Meron, D. *et al*. Role of flagella in virulence of the coral pathogen *Vibrio*
633 *coralliilyticus*. *Appl. Environ. Microbiol.* **75**, 5704-5707 (2009).

634 47. Ushijima, B. *et al*. Vibrio coralliilyticus strain OCN008 is an etiological agent of
635 acute Montipora white syndrome. *Appl. Environ. Microbiol.* **80**, 2102-2109 (2014).

636 48. Butler, S. M. & Camilli, A. Going against the grain: chemotaxis and infection in
637 Vibrio cholerae. *Nature reviews Microbiology* **3**, 611 (2005).

638 49. O'Toole, R., Milton, D. L. & Wolf-Watz, H. Chemotactic motility is required for
639 invasion of the host by the fish pathogen Vibrio anguillarum. *Mol. Microbiol.* **19**, 625-
640 637 (1996).

641 50. Stocker, R. The 100 μm length scale in the microbial ocean. *Aquat. Microb. Ecol.*
642 **76**, 189-194 (2015).

643 51. Shapiro, O. H. *et al*. Vortical ciliary flows actively enhance mass transport in reef
644 corals. *Proceedings of the National Academy of Sciences* **111**, 13391-13396 (2014).

645 52. Katz, S. M., Pollock, F. J., Bourne, D. G. & Willis, B. L. Crown-of-thorns starfish
646 predation and physical injuries promote brown band disease on corals. *Coral Reefs*
647 **33**, 705-716 (2014).

648 53. Nugues, M. M. & Bak, R. P. Differential competitive abilities between Caribbean
649 coral species and a brown alga: a year of experiments and a long-term perspective.
650 *Mar. Ecol. Prog. Ser.* **315**, 75-86 (2006).

651 54. Kramarsky-Winter, E. *et al*. The possible role of cyanobacterial filaments in coral
652 black band disease pathology. *Microb. Ecol.* **67**, 177-185 (2014).

653 55. Agostini, S. *et al*. Biological and chemical characteristics of the coral gastric cavity.
654 *Coral Reefs* **31**, 147-156 (2012).

655 56. Houlbrèque, F., Rodolfo-Metalpa, R. & Ferrier-Pagès, C. Heterotrophic Nutrition of
656 Tropical, Temperate and Deep-Sea Corals. *Diseases of Coral*, 150-163 (2015).

657 57. Sorokin, Y. I. Trophical role of bacteria in the ecosystem of the coral reef. *Nature*
658 **242**, 415-417 (1973).

659 58. Krediet, C. J., Ritchie, K. B., Paul, V. J. & Teplitski, M. Coral-associated micro-
660 organisms and their roles in promoting coral health and thwarting diseases. *Proc.*
661 *Biol. Sci.* **280**, 20122328 (2013).

662 59. Sato, Y., Civiello, M., Bell, S. C., Willis, B. L. & Bourne, D. G. Integrated approach to
663 understanding the onset and pathogenesis of black band disease in corals. *Environ.*
664 *Microbiol.* **18**, 752-765 (2016).

665 60. Rosenberg, E., Sharon, G. & Zilber-Rosenberg, I. The hologenome theory of
666 evolution contains Lamarckian aspects within a Darwinian framework. *Environ.*
667 *Microbiol.* **11**, 2959-2962 (2009).

668 61. Barshis, D. J. *et al*. Genomic basis for coral resilience to climate change. *Proc. Natl.*
669 *Acad. Sci. U. S. A.* **110**, 1387-1392 (2013).

670 62. Palumbi, S. R., Barshis, D. J., Traylor-Knowles, N. & Bay, R. A. Mechanisms of reef
671 coral resistance to future climate change. *Science* **344**, 895-898 (2014).

672 63. Wilson, B. *et al*. An improved detection and quantification method for the coral
673 pathogen Vibrio coralliilyticus. *PloS one* **8**, e81800 (2013).

674 64. Certner, R. H., Dwyer, A. M., Patterson, M. R. & Vollmer, S. V. Zooplankton as a
675 potential vector for white band disease transmission in the endangered coral,
676 Acropora cervicornis. *PeerJ* **5**, e3502 (2017).